Effect of spin-polarized electrons on terahertz emission from photoexcited GaAs

James M. Schleicher, Shayne M. Harrel, and Charles A. Schmuttenmaer[a)]
Department of Chemistry, Yale University, 225 Prospect St., New Haven, Connecticut 06520-8107, USA

(Received 21 December 2008; accepted 5 April 2009; published online 5 June 2009)

The influence of elliptically and circularly polarized excitation on terahertz emission from unbiased bulk GaAs at normal incidence and room temperature is reported. Illumination of GaAs above the bandgap produces both spin-polarized electrons and shift currents. The induced currents are monitored via terahertz emission spectroscopy. The terahertz emission amplitude is compared to theoretical calculations as a function of excitation beam ellipticity. Exciting slightly above the bandgap (800 nm at room temperature) with elliptical polarization generates shift currents that deviate substantially from theoretical predictions. On the other hand, exciting either below the bandgap (835 nm at 77 K) to produce optical rectification or far above the bandgap (400 nm at room temperature) to produce shift currents generates emission in agreement with theoretical calculations. Spin-polarized electrons created by elliptically polarized excitation are the source of the observed discrepancy. © *2009 American Institute of Physics*. [DOI: 10.1063/1.3133093]

I. INTRODUCTION AND BACKGROUND

Using photons to control electrical currents is of great interest in photonics since it affords the ultimate in switching speeds. In addition, the ability to observe and manipulate both spins and currents is necessary to advance the field of spintronics. This paper describes the influence of spin-polarized electrons on shift currents in bulk unbiased GaAs at normal incidence and room temperature.

The first terahertz emissions from unbiased bulk GaAs were reported by Zhang and co-workers.[1] Zhang and co-workers then mapped out the terahertz emission dependence on azimuthal angle when illuminating the (111) and (110) crystal faces of semi-insulating GaAs.[2–4] The azimuthal dependence was plotted for linearly polarized excitation parallel and perpendicular to the terahertz detector axis. Terahertz emission has also been observed from coherent control of photocurrent in bulk unbiased low-temperature grown GaAs.[5,6] This coherent control is achieved by varying the relative phase of excitation beams that drive the one-photon and two-photon interband absorptions.

Sipe and Shkrebtii[7] derived an expression for the second-order susceptibility tensor $\chi^{(2)}$ and performed a full band-structure calculation for GaAs. Nastos and Sipe[8] then published the most complete theoretical treatment of terahertz response below and above the bandgap. Their report calculates the electronic contribution to the nonlinear susceptibility over a range of central frequencies enabling the electronic response to a femtosecond laser pulse to be determined. These two reports demonstrate that the above bandgap response is dominated by a shift current component that is two orders of magnitude larger than the optical rectification per unit path length, and the below bandgap emission is generated solely by optical rectification.

In GaAs, the electron density at the top of the valence band Γ_8 point is localized primarily around the As atoms. At the lowest point of the Γ_6 conduction band, the electron density is localized around the Ga atoms.[8] Due to the lack of inversion symmetry in GaAs, a resonant optical transition may cause a shift in the center of charge in the unit cell. However, whether or not optical excitation yields a current (and therefore terahertz emission) depends on the polarization of the excitation beam and crystal face that is illuminated. For example, illuminating GaAs(111) with light polarized linearly along one of the (111) crystal axes yields a shift current where the electron moves from the As atom to the particular Ga atom that is located along the direction of the polarization. Alternatively, illuminating GaAs(100) with any polarization yields no shift current as the electrons have equal probability of moving to any of its four nearest neighbors.

Until now, no report exists detailing the dependence of terahertz emission on elliptical and circular polarization at normal incidence for any of the terahertz generation mechanisms in GaAs, although Nastos *et al.*[9] recently reported terahertz generation using circularly polarized light at non-normal incidence.

II. EXPERIMENTAL

All data presented in this paper were recorded using the experimental setup described previously[10] (see the supplementary information for a schematic diagram[11]). Briefly, >99% of laser intensity (1 kHz pulse train of ~100 fs pulses at ~800 mW average power) initiates a process that produces a terahertz pulse. The emission is detected by free-space electro-optic sampling (FSEOS) using a 1 mm thick ZnTe(110) crystal where the remaining <1% of the optical beam serves as an optical gate.[12] Manipulation of the excitation beam polarization is achieved by placing half- and quarter-wave plates (both zero order) in the excitation beam path. Data reported as a function of wave plate angle are obtained by measuring only the peak of the waveform and

[a)]Electronic mail: charles.schmuttenmaer@yale.edu.

 © 2009 American Institute of Physics

Downloaded 07 Jul 2009 to 130.132.248.62. Redistribution subject to AIP license or copyright; see http://jap.aip.org/jap/copyright.jsp

averaging at least 500 points. Recording the terahertz amplitude retains phase information, which is critical to determining the direction of the current within the sample (any power detector such as a bolometer would be unable to differentiate between currents moving in opposite directions). In addition, FSEOS is a polarization sensitive detection technique, which allows explicit detection of emission in *X*- and *Y*-directions, enabling two-dimensional mapping of the terahertz emission, and therefore the actual direction of the underlying rectification and shift currents. Two additional advantages of using terahertz emission spectroscopy instead of electrical measurements are that rectification and shift currents are easily distinguishable based on the shape of the waveform, and no electrodes need be deposited on the samples.

GaAs is a III-V compound semiconductor with a zinc blende structure. Studies reported here were performed on GaAs(111) and GaAs(110) crystal orientations. The wafers were purchased from Litton with additional samples of GaAs(111) purchased from AXT, Inc. The *X*-emission for GaAs(111) is defined as the component of the terahertz emission that is parallel to the projection of the (100) axis onto the surface of the wafer, and for GaAs(110) the *X*-emission is defined as the component parallel to the (001) axis (see supplementary information for more details[11]). The *Y*-emission for both crystal faces is perpendicular to the *X*-emission. Samples were mounted in a Janis optical cryostat (evacuated to ~30 mTorr) and illuminated under three conditions: below bandgap (at 77 K with 835 nm excitation), slightly above bandgap (at room temperature with 800 nm excitation), and far above bandgap (at room temperature with 400 nm excitation). The data reported use the following notation: "emission direction"/"above or below" (e.g., *X*/above indicates *X*-polarized emission and above bandgap excitation). The excitation polarization prior to the quarter-wave plate was either parallel or perpendicular to the *X*-emission direction, with perpendicular indicated by the presence of an asterisk, i.e., *X*/above*. In GaAs(111), the behavior was identical in each of these cases due to symmetry, so only data taken with parallel input polarization need be reported.

When exciting GaAs with light that is either elliptically or circularly polarized with photon energy of 0.34 eV or less above the bandgap (between 1.43 and 1.77 eV at room temperature), an excess of spin-polarized electrons is generated (see Refs. 13–15 and the supplementary information for more details[11]). Since our excitation wavelength for probing the slightly above bandgap response is 800 nm (~1.55 eV), spin-polarized electrons are generated when exciting with elliptical or circular polarization. Furthermore, the spin-polarized electron population will vary sinusoidally as a function of the angle between the quarter-wave plate and the input beam's linear polarization with a period of 180°, i.e., zero when excitation beam is linear, a maximum amount when circular, and opposite spin polarization for opposite handedness of the excitation beam.

III. RESULTS AND DISCUSSION

The zinc blende structure lacks inversion symmetry, so the lowest-order nonlinear contribution to the susceptibility is second order, i.e., $\chi^{(2)}$. All matter-field interactions that vary as the second power of the electric field strength are described by $\chi^{(2)}$. Sipe and Skrebtii[7] showed that when a pulse of light with central frequency ω_o and a time-varying electric field defined by

$$E(t) = \int_{-\infty}^{\infty} d\omega \tilde{E}(\omega) e^{-i(\omega-\omega_o)t} \tag{1}$$

[where $\tilde{E}(\omega)$ are the Fourier components] interacts with a semiconductor, the induced nonlinear polarization is defined as

$$\tilde{P}^{(2)}(\Omega) \propto \chi^{(2)} \tilde{E}(\omega) \tilde{E}(\omega - \Omega), \tag{2}$$

where the second-order susceptibility has the general form

$$\chi^{(2)}(-\Omega;\omega,-\omega+\Omega) = \chi^{(2)\prime}(-\Omega;\omega,-\omega+\Omega) + \frac{\sigma^{(2)}(-\Omega;\omega,-\omega+\Omega)}{i\Omega} + \frac{\eta^{(2)}(-\Omega;\omega,-\omega+\Omega)}{(-i\Omega)^2}, \tag{3}$$

where ω is the optical frequency, Ω is the terahertz frequency, and $\Omega \ll \omega$. The first term represents the optical rectification component, the second represents the shift current component, and the third represents the injection current. Injection currents are forbidden by symmetry in zinc blende crystals and can thus be ignored.

The terahertz emission from shift currents $E_{\text{shift}}(t)$ detected in the far field (see Ref. 16) varies as a function of time as

$$E_{\text{shift}}(t) \propto \frac{\partial}{\partial t}[E_{\text{vis}}(t) E^*_{\text{vis}}(t)], \tag{4}$$

and the emission from optical rectification $E_{\text{rect}}(t)$ varies with time as

$$E_{\text{rect}}(t) \propto \frac{\partial^2}{\partial t^2}[E_{\text{vis}}(t) E^*_{\text{vis}}(t)], \tag{5}$$

where $E_{\text{vis}}(t)E^*_{\text{vis}}(t)$ is essentially the excitation pulse intensity envelope.[7] The first-derivative relationship between, above, and below bandgap emission was previously observed,[17] but the presence of focusing optics in that experiment did not allow the temporal profile of the emission to be related to the excitation pulse. The terahertz emission from GaAs(111) is shown in Fig. 1 for linear excitation slightly above and below the bandgap (taken in the far field). The numerical first and second derivatives of a Gaussian waveform (the shape of our optical pulse intensity envelope) having a full width at half maximum of 700 fs (our instrument response time for 100 fs pulses) are shown for comparison. There is excellent agreement in the observed signal with that calculated by Sipe and Skrebtii:[7] the above bandgap excitation (shift current) produces a terahertz transient varying as the first derivative of the optical pulse envelope, while a second derivative line shape is obtained when exciting below the bandgap (optical rectification). The time-derivative relationship between terahertz emission from actual currents,

Downloaded 07 Jul 2009 to 130.132.248.62. Redistribution subject to AIP license or copyright; see http://jap.aip.org/jap/copyright.jsp

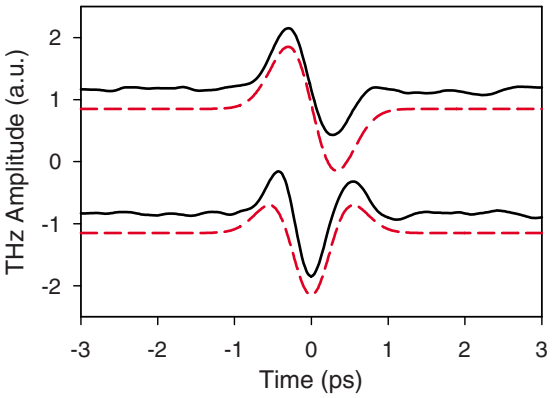

FIG. 1. (Color online) Top: experimental (black/solid) and calculated emission (red/dashed) for above bandgap excitation. Bottom: experimental (black/solid) and calculated emission (red/dashed) for below bandgap excitation. The experimental data are vertically offset from the calculation for clarity. Relative vertical offset of the pairs of traces is arbitrary.

such as when voltage-biased electrodes are used, versus optical rectification has been noted by Wynne and Carey[18] using a phenomenological model.

The *X*/below and *Y*/below data sets for GaAs(111), as well as those obtained when exciting far above the bandgap with 400 nm excitation, are shown in Fig. 2. They show excellent agreement with the theoretical predictions [as do the results for GaAs(110), which are found in supplementary information Figs. S4 and S5 (Ref. 11)]. Data sets taken with excitation slightly above the bandgap are shown in Fig. 3 for GaAs(111) [*X*/above in Fig. 3(a) and *Y*/above in Fig. 3(d)] and GaAs(110) [*X*/above in Fig. 3(b), *Y*/above in Fig. 3(e), *X*/above* in Fig. 3(c), and *Y*/above* in Fig. 3(f)]. There is obvious disagreement between the calculated behavior and these experimental data sets.

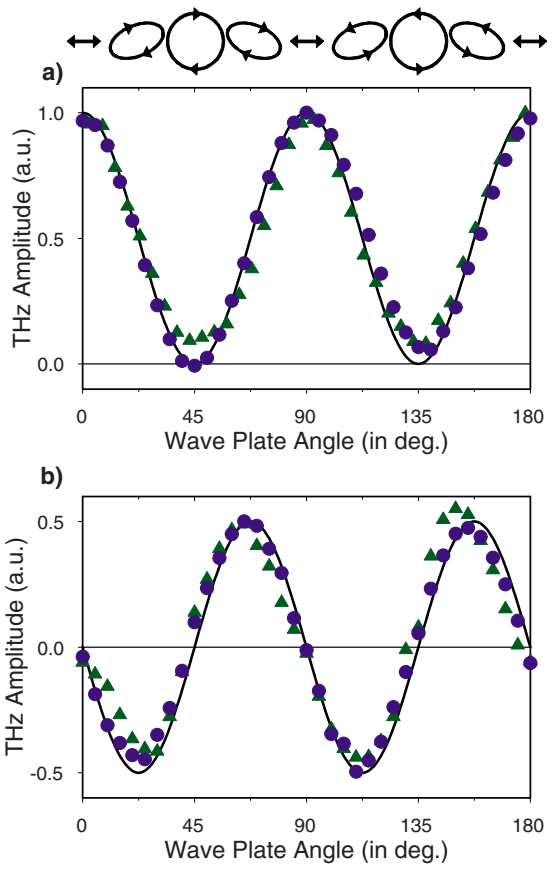

FIG. 2. (Color online) Terahertz emission dependence on quarter-wave plate angle for excitation below bandgap (green triangles) and far above bandgap at 400 nm (blue circles) plotted with theoretical calculations (solid black curve). The *X*-emission is shown in (a) and the *Y*-emission is shown in (b). The ellipticity and handedness of the light at select angles have been graphically represented at the very top.

Terahertz emission, whether exciting slightly above the bandgap or not, is calculated to be independent of the handedness of an elliptically polarized excitation beam. That is, as the quarter-wave plate is rotated from 0° to 90° (right-handed polarization), the emission is calculated to be identical to that when the wave plate is rotated from 90° to 180° (left-handed polarization). Passing light through a quarter-wave plate with its optic axis set at angles θ and $\theta \pm 90°$ relative to the incoming optical linear polarization results in identical ellipticity but opposite handedness (see the depiction at the top of Fig. 2). The measured data in Fig. 3 show a dramatic dependence on the handedness of the light (for the same ellipticity) when exciting slightly above the bandgap. Instead of *X*- and *Y*-emissions for each orientation repeating in the fashion expected, the *X*-emission from 0° to 90° repeats as the wave plate is rotated from 180° back to 90°. That is, there is symmetry about 90° where angles of $90° \pm \theta$ have a response of the same magnitude and sign. The *Y*-emission as a function of angle from 0° to 90° also repeats as the wave plate is rotated from 180° back to 90° but with opposite sign. That is, angles of $90° \pm \theta$ have a response of the same magnitude but opposite polarity.

This dependence on handedness is caused by spin-polarized electrons altering the shift current trajectory and is supported by the following observations. First, the effect is only observed when spin-polarized electrons are present. The data taken with excitation far above the bandgap agree almost perfectly with calculations and represent the true shift current response. In addition, the emission due to optical rectification also agrees with the calculations. Second, by purchasing wave plates from multiple vendors, we have verified that the behavior is not due to an imperfect wave plate. Furthermore, regardless of the retardation of the wave plate, the calculated response from 0° to 90° will always be identical to that from 90° to 180°, so an imperfect quarter-wave plate cannot produce the behavior we see. Finally, we have eliminated the possibility that an artifact of crystal growth conditions is causing this behavior by purchasing GaAs wafers from two vendors, as stated in Sec. II. We also note that this behavior is not due to surface effects because the optical skin depth of GaAs is about 700 nm for 800 nm light and only 15 nm for 400 nm light.[19] If surface effects were important, they would influence the 400 nm excitation data far more than when exciting at 800 nm, which is contrary to our observations.

Because we detect both *X*-polarized and *Y*-polarized terahertz emissions, it is possible to construct a polar plot that reveals the actual in-plane magnitude and direction of the current flow. Figure 4 displays this for the measured and calculated GaAs(111) response, and the data sets for GaAs(110) in orientations of *X*/above, *Y*/above, *X*/above*,

Downloaded 07 Jul 2009 to 130.132.248.62. Redistribution subject to AIP license or copyright; see http://jap.aip.org/jap/copyright.jsp

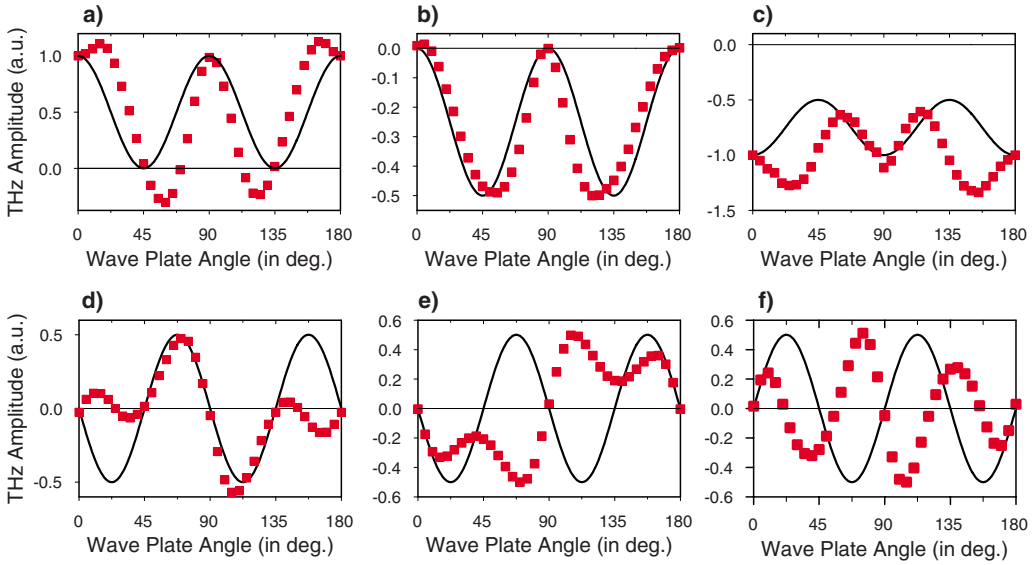

FIG. 3. (Color online) Terahertz emission dependence on quarter-wave plate angle for excitation slightly above the bandgap (red squares) plotted with theoretical calculations (solid black curve). For GaAs(111): (a) *X*/above and (d) *Y*/above. For GaAs(110): (b) *X*/above, (c) *X*/above*, (e) *Y*/above, and (f) *Y*/above*.

and *Y*/above* are found in the supplementary information Fig. S7.[10] Two important quantities are shown in Fig. 4. (1) The amount of rotation from the calculated current direction (shown with the black vector) toward the direction of the actual current, as given by the angle ϕ between the black vector and red dashed vector, or ϕ', the angle between the black vector and blue dashed vector. The red and blue dashed vectors are the measured direction of the shift current for a quarter-wave plate setting of 60° and 150°, respectively. The black vector is the direction of the shift current in the absence of spin-polarized electrons for either of these wave plate settings. (2) The magnitude and direction of the *difference* vector that connects the two, as shown by the red and blue dotted arrows for 60° and 150°, respectively.

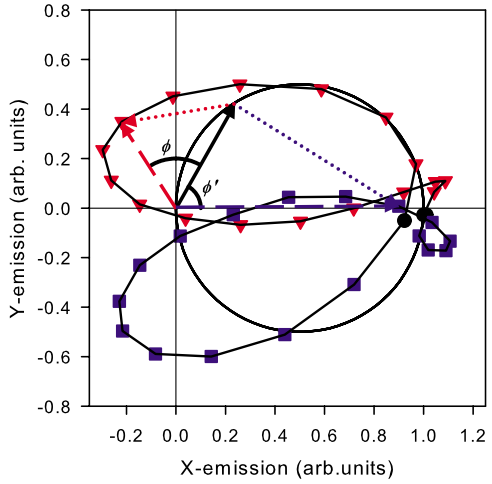

FIG. 4. (Color online) Polar plot representing the current within the plane of GaAs(111) as a quarter-wave plate is rotated. The thick solid black line forming a circle represents the calculated current: twice repeating, one full clockwise loop as the wave plate is rotated from 0° to 90°, and a second as it is rotated from 90° to 180°. Both begin and end at an *X*-emission of 1 and a *Y*-emission of 0. The red triangles represent right-handed excitation (wave plate angles from 5° to 85°), blue squares represent left-handed excitation (from 95° to 175°), and black circles represent linear excitation (0°, 90°, and 180°). The solid black vector is the predicted response for a pair of quarter-wave plate angles that give excitation of opposite handedness but with the same predicted current (60° and 150°). The red dashed line, offset from the predicted response by the angle ϕ, represents the measured current at 60° and the blue dashed line, offset by the angle ϕ', represents the current at 150°. The red and blue dotted lines (corresponding again to the offsets represented by angles ϕ and ϕ', respectively) are the vector differences.

The first quantity (amount of rotation) indicates the angular deviation in the shift current when spin-polarized electrons are present. The second quantity (difference vector) is a measure of the additional current that arises when spin-polarized electrons are present to generate the deviation (that is, the difference of the observed direction and magnitude of shift current versus that which is calculated).

Figure 5 displays the difference in angle or direction of the current that flows in the presence of spin-polarized electrons versus their absence. Part (a) displays the result for GaAs(111) where it is seen that the deviation follows a nearly sinusoidal pattern in agreement with the magnitude and direction of the magnetic field produced by the photogenerated spin-polarized electrons (the spikes at 45° and 135° are spurious because there is essentially no current at these wave plate angles). In fact, one can construct a model to replicate the observed behavior based on the Lorentz equation $F=q_oE+q_ov\times B$, where q_0 is the charge of the carrier, v is its velocity, E in our case represents the field that drives the shift current, and B is the magnetic field arising from the spin-polarized electrons. However, as seen in parts (b) and (c), the behavior is radically different for GaAs(110) samples. In part (c) the direction of the rotation actually changes sign even when spin-polarized electrons are oriented in the same direction. Therefore, we conclude that while spin-polarized electrons are responsible for the deviation between the expected shift currents and those measured, it is not a simple "Hall effect" mechanism.

Figure 6 examines the magnitude and direction of the vector representing the additional current generated by having spin-polarized electrons present (the dotted lines in Fig.

Downloaded 07 Jul 2009 to 130.132.248.62. Redistribution subject to AIP license or copyright; see http://jap.aip.org/jap/copyright.jsp

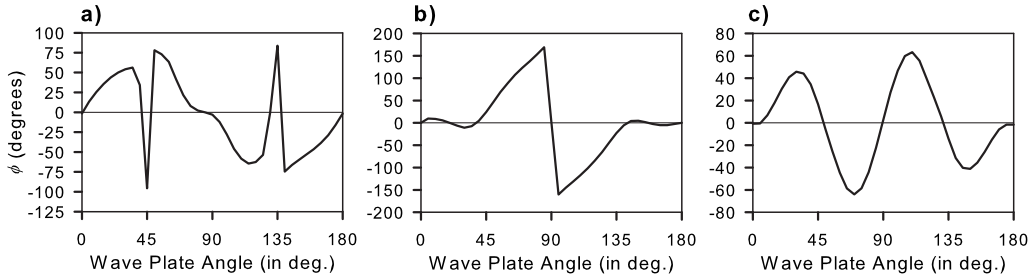

FIG. 5. The angle of rotation (ϕ) between the predicted shift current response and that measured slightly above the bandgap plotted as a function of quarter-wave plate angle. The data are (a) GaAs(111), (b) GaAs(110) with initial excitation polarization parallel to the *X*-emission axis, and (c) GaAs(110) with initial excitation polarization perpendicular to the *X*-emission axis.

4). Here, the ξ is the angle of the difference vector relative to lab-fixed axes (not the angle of rotation ϕ between the observed minus calculated vectors) and R is its magnitude. One of the most striking features is that there are reasonably well defined angles within the samples that the additional current flows. This is evident in both the ξ plots [Figs. 6(a)–6(c)] and polar plots [Figs. 6(g)–6(i)]. The polar plot for the (111) sample [Fig. 6(g)] appears to be related to the underlying crystal structure, but this is not the case for the (110) sample [Figs. 6(h) and 6(i)]. Furthermore, the preferred angles in the (110) sample depend on whether the excitation beam is horizontally or vertically polarized prior to the quarter-wave plate, as seen by comparing Figs. 6(h) and 6(i). This indicates a complex interplay between the optical field and crystallographic structure.

Figure 7 displays the results of applying an external magnetic field when generating shift currents with a linearly polarized excitation beam (where no spin-polarized electrons are present). When the shift current is perpendicular to the detector axis no signal is observed, as shown with the solid black line. However, an external magnetic field alters the current and rotates it onto the axis that the detector is sensitive to. Reversing the direction of the magnet reverses the direction of the current. These observations are consistent

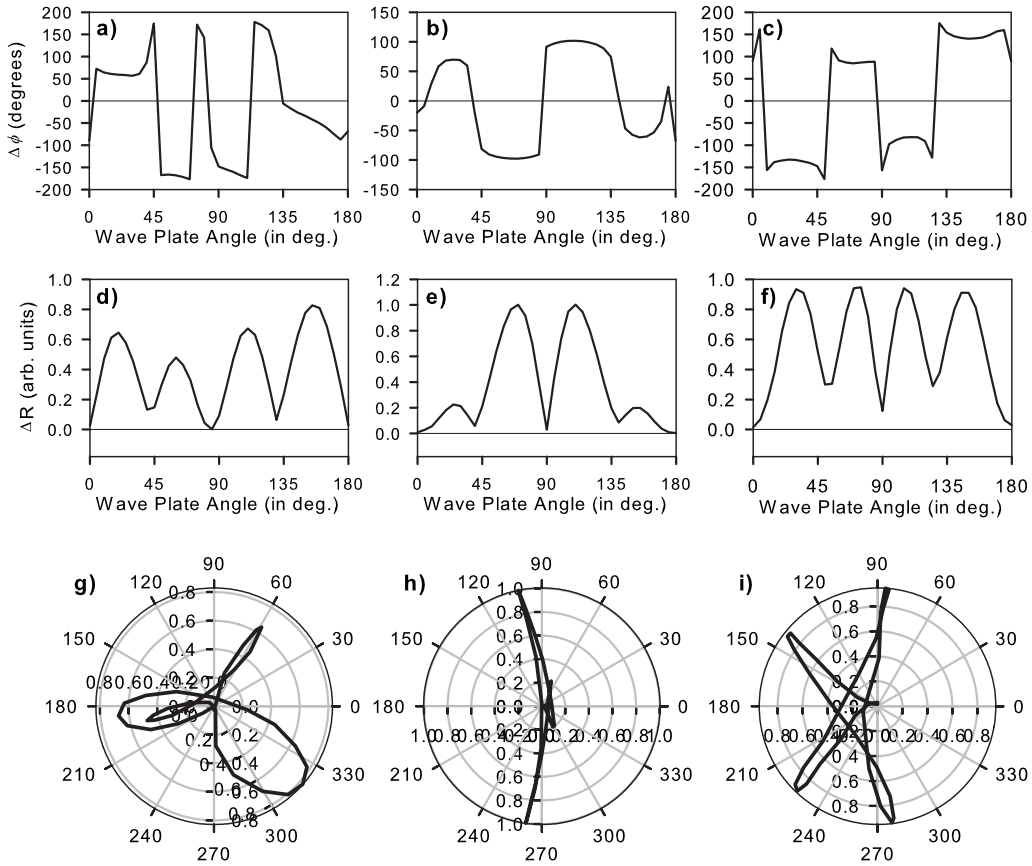

FIG. 6. The vector difference between the predicted shift current response and the measured shift current response (represented graphically as the dotted arrow in Fig. 4). ξ represents the angle of that vector difference in degrees [(a)–(c)], R represents the length in arbitrary units [(d)–(f)], and the polar plots are a combination of those values plotted in two dimensions [(g)–(i)]. The graphs correspond to GaAs(111) [(a), (d), and (g)], GaAs(110) with initial excitation polarization parallel to the *X*-emission axis [(b), (e), and (h)], and GaAs(110) with initial excitation polarization perpendicular to the *X*-emission axis [(c), (f), and (i)].

Downloaded 07 Jul 2009 to 130.132.248.62. Redistribution subject to AIP license or copyright; see http://jap.aip.org/jap/copyright.jsp

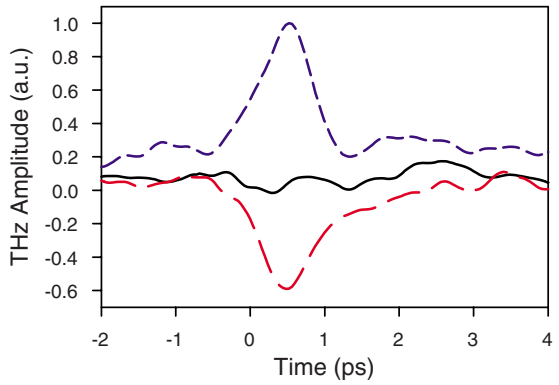

FIG. 7. (Color online) Terahertz emission from shift currents perpendicular to the detector axis under the influence of no magnetic field (black/solid) with a strong permanent magnet near the surface (red/long dashed) and with that same magnet flipped to apply the opposite field (blue/short dashed).

with carriers moving within a semiconductor subject to a Lorentz force and demonstrate that shift currents are actual currents.

IV. CONCLUSIONS

These are one color experiments in bulk materials at normal incidence without applied electric or magnetic fields (except for the results shown in Fig. 7). This behavior is fundamentally different from other phenomena that seem to be likely candidates for the observed behavior such as spin-Hall effect, anomalous Hall effect (AHE), photo-Hall effect, and magnetogyrotropic photogalvanic effect (MPGE), as compared in Table I.

We have also verified the first and second time-derivative relationships among the excitation pulse, shift current, and optical rectification. Also, shift currents are real currents and their trajectories can be influenced by an external magnetic field.

The terahertz emission dependence on elliptical and circular polarizations is reported for GaAs(111) and GaAs(110) when photoexciting below, slightly above, and far above the bandgap. The below and far above bandgap data sets agree with theoretical calculations, while slightly above bandgap excitation gives extreme variations within all data sets. These variations depend on spin-polarized electrons in a nonintuitive manner, and the observed behavior might best be described as a time-dependent, optical AHE phenomenon. In any case, it is certainly due to spin-orbit coupling,[20] and future work will provide a microscopic understanding.

TABLE I. A succinct comparison of possible candidates for the observed behavior.

Phenomenon	Applied E field	Applied B field	Comments
Spin-Hall effect	Yes	No	Spin current only
Anomalous Hall effect	Yes	Usually	Ferromagnets
Photo-Hall effect	Yes	Yes	Photogeneration of carriers
MPGE	No	No	Strained quantum wells
This work	No	No	Bulk material

ACKNOWLEDGMENTS

We acknowledge the National Science Foundation (Grant No. CHE-0616875) for partial support of this work.

APPENDIX: LASER POLARIZATION DEPENDENCE OF SECOND-ORDER RESPONSE

The terahertz pulse generated due to optical rectification or shift currents depends on the polarization state of the laser (linear, elliptical, or circular) and the orientation of the sample. We employ the Jones matrix formalism to account for various optics and sample orientation.[21] In this formalism, the elements of the vectors and matrices below are complex quantities. The initial polarization of the optical beam is written as

$$\boldsymbol{E}_{\mathrm{lab}} = \begin{bmatrix} E_{x,\mathrm{opt}} \\ E_{y,\mathrm{opt}} \\ E_{z,\mathrm{opt}} \end{bmatrix}, \tag{A1}$$

where x, y, and z are laboratory fixed coordinates. The z-direction is the direction of propagation, and we can arbitrarily choose the x-direction as horizontal and y as vertical. Thus, a horizontally, linearly polarized beam emerging from the laser is represented as

$$\boldsymbol{E}_{\mathrm{lab}} = \begin{bmatrix} 1 \\ 0 \\ 0 \end{bmatrix}. \tag{A2}$$

When the beam passes through a wave plate, the polarization state of the emerging beam is expressed as

$$\boldsymbol{E}'_{\mathrm{lab}} = \begin{bmatrix} E_{x',\mathrm{opt}} \\ E_{y',\mathrm{opt}} \\ E_{z',\mathrm{opt}} \end{bmatrix} = \mathbf{W} \begin{bmatrix} E_{x,\mathrm{opt}} \\ E_{y,\mathrm{opt}} \\ E_{z,\mathrm{opt}} \end{bmatrix} = \mathbf{W}\boldsymbol{E}_{\mathrm{lab}}, \tag{A3}$$

where $\mathbf{W}$ is the product of the matrices

$$\mathbf{W} = \mathbf{R}(-\theta)\mathbf{W}_0\mathbf{R}(\theta) \tag{A4}$$

with

$$\mathbf{W}_0 = e^{-i\phi} \begin{bmatrix} e^{-i\Gamma/2} & 0 & 0 \\ 0 & e^{i\Gamma/2} & 0 \\ 0 & 0 & 1 \end{bmatrix} \tag{A5}$$

and

$$\mathbf{R}(\theta) = \begin{bmatrix} \cos\theta & \sin\theta & 0 \\ -\sin\theta & \cos\theta & 0 \\ 0 & 0 & 1 \end{bmatrix}. \tag{A6}$$

$\mathbf{W}_0$ is the matrix describing the phase retardation placed on the optical beam where Γ equals π for a half-wave plate or $\pi/2$ for a quarter-wave plate. $\mathbf{R}(\theta)$ is a rotation matrix that transforms the incident optical beam onto the fast and slow axes of the wave plate, and θ is the angle of the optical beam with respect to the fast axis. The emerging beam is then transformed back into laboratory coordinates using $\mathbf{R}(-\theta)$ and carries the polarization induced by the wave plate.

Downloaded 07 Jul 2009 to 130.132.248.62. Redistribution subject to AIP license or copyright; see http://jap.aip.org/jap/copyright.jsp

The optical field is then projected onto the crystallographic axis of the sample

$$\boldsymbol{E}_{\mathrm{xtal}} = \begin{bmatrix} E_i \\ E_j \\ E_k \end{bmatrix} = \mathbf{T} \begin{bmatrix} E_{x'} \\ E_{y'} \\ E_{z'} \end{bmatrix} = \mathbf{T}\boldsymbol{E}'_{\mathrm{lab}}, \tag{A7}$$

where $\mathbf{T}$ is the transformation matrix projecting the electric field in laboratory coordinates onto the i, j, and k crystallographic axes of the GaAs(111) or GaAs(110) sample

$$\mathbf{T}_{(111)} = \begin{bmatrix} \sqrt{\frac{2}{3}} & 0 & \frac{1}{\sqrt{3}} \\ -\frac{1}{\sqrt{6}} & \frac{1}{\sqrt{2}} & \frac{1}{\sqrt{3}} \\ -\frac{1}{\sqrt{6}} & -\frac{1}{\sqrt{2}} & \frac{1}{\sqrt{3}} \end{bmatrix}, \tag{A8}$$

$$\mathbf{T}_{(110)} = \begin{bmatrix} 1 & 0 & 0 \\ 0 & \frac{1}{\sqrt{2}} & \frac{1}{\sqrt{2}} \\ 0 & -\frac{1}{\sqrt{2}} & \frac{1}{\sqrt{2}} \end{bmatrix}. \tag{A9}$$

For zinc blende crystals such as GaAs, the induced polarization or "current" in the ith direction is proportional to the product of the optical fields polarized along the jth and kth directions: $P_i \propto E_j E_k^*$, where i, j, and k are mutually orthogonal Cartesian coordinates and E^* is the complex conjugate of E,[4,22]

$$\boldsymbol{P} = \begin{bmatrix} 0 & 0 & E_j \\ E_k & 0 & 0 \\ 0 & E_i & 0 \end{bmatrix} \begin{bmatrix} E_i^* \\ E_j^* \\ E_k^* \end{bmatrix} = \begin{bmatrix} 0 & 0 & E_j \\ E_k & 0 & 0 \\ 0 & E_i & 0 \end{bmatrix} \boldsymbol{E}_{\mathrm{xtal}}^*. \tag{A10}$$

This time-dependent polarization leads to the observed terahertz emission which is transformed back into laboratory coordinates

$$\boldsymbol{E}_{\mathrm{THz}} = \begin{bmatrix} E_{x,\mathrm{THz}} \\ E_{y,\mathrm{THz}} \\ E_{z,\mathrm{THz}} \end{bmatrix} = \mathbf{T}^{-1} \begin{bmatrix} P_i \\ P_j \\ P_k \end{bmatrix} = \mathbf{T}^{-1}\boldsymbol{P}, \tag{A11}$$

where $\mathbf{T}^{-1}$ is the inverse of the transformation matrix $\mathbf{T}$. Putting this together, we have

$$\boldsymbol{E}_{\mathrm{THz}} = \mathbf{T}^{-1}\boldsymbol{P}\mathbf{T}\mathbf{R}(-\theta)\mathbf{W}_0\mathbf{R}(\theta)\boldsymbol{E}_{\mathrm{lab}}, \tag{A12}$$

and the calculated signal is obtained by taking the real part of $\boldsymbol{E}_{\mathrm{THz}}$ in Eq. (A12).

If we were to rotate the sample instead of the wave plate, as many other workers have done,[4] this same type of analysis would lead to

$$\boldsymbol{E}_{\mathrm{THz}} = \mathbf{R}(-\theta)\mathbf{T}^{-1}\boldsymbol{P}\mathbf{T}\mathbf{R}(\theta)\boldsymbol{E}_{\mathrm{lab}}. \tag{A13}$$

In summary, the Jones matrix formalism[21] is a well-known and efficient way to describe and understand the effects of essentially any optical element as well as the samples themselves.

[1] B. B. Hu, X. C. Zhang, and D. H. Auston, Phys. Rev. Lett. **67**, 2709 (1991).
[2] X. C. Zhang, Y. Jin, and X. F. Ma, Appl. Phys. Lett. **61**, 2764 (1992).
[3] X.-C. Zhang, Y. Jin, K. Ware, X. F. Ma, A. Rice, D. Bliss, J. Larkin, and M. Alexander, Appl. Phys. Lett. **64**, 622 (1994).
[4] A. Rice, Y. Jin, X. F. Ma, X.-C. Zhang, D. Bliss, J. Larkin, and M. Alexander, Appl. Phys. Lett. **64**, 1324 (1994).
[5] A. Hache, Y. Kostoulas, R. Atanasov, J. L. P. Hughes, J. E. Sipe, and H. M. van Driel, Phys. Rev. Lett. **78**, 306 (1997).
[6] A. Hache, J. E. Sipe, and H. M. van Driel, IEEE J. Quantum Electron. **34**, 1144 (1998).
[7] J. E. Sipe and A. I. Shkrebtii, Phys. Rev. B **61**, 5337 (2000).
[8] F. Nastos and J. E. Sipe, Phys. Rev. B **74**, 035201 (2006).
[9] F. Nastos, R. W. Newson, J. Hubner, H. M. van Driel, and J. E. Sipe, Phys. Rev. B **77**, 195202 (2008).
[10] E. Beaurepaire, G. M. Turner, S. M. Harrel, M. C. Beard, J.-Y. Bigot, and C. A. Schmuttenmaer, Appl. Phys. Lett. **84**, 3465 (2004).
[11] See EPAPS Document No. E-JAPIAU-105-116910 for additional material on the experimental apparatus, wafer orientation, and definition of axes generating spin-polarized electrons, excitation of GaAs(110) well above the bandgap, and additional polar plots. For more information on EPAPS, see http://www.aip.org/pubservs/epaps.html.
[12] Q. Wu and X. C. Zhang, Appl. Phys. Lett. **67**, 3523 (1995).
[13] G. Lampel, Phys. Rev. Lett. **20**, 491 (1968).
[14] D. T. Pierce and F. Meier, Phys. Rev. B **13**, 5484 (1976).
[15] D. T. Pierce, R. J. Celotta, G.-C. Wang, W. N. Unertl, A. Galejs, C. E. Kuyatt, and S. R. Mielczarek, Rev. Sci. Instrum. **51**, 478 (1980).
[16] A. E. Kaplan, J. Opt. Soc. Am. B **15**, 951 (1998).
[17] D. Cote, N. Laman, and H. M. van Driel, Appl. Phys. Lett. **80**, 905 (2002).
[18] K. Wynne and J. J. Carey, Opt. Commun. **256**, 400 (2005).
[19] D. E. Aspnes and A. A. Studna, Phys. Rev. B **27**, 985 (1983).
[20] N. A. Sinitsyn, J. Phys.: Condens. Matter **20**, 023201 (2008).
[21] Y. Yariv and P. Yeh, *Optical Waves in Crystals: Propagation and Control of Laser Radiation* (Wiley, New York, 1984).
[22] P. N. Butcher and D. Cotter, *The Elements of Nonlinear Optics* (Cambridge University Press, Cambridge, England, 1990).

Downloaded 07 Jul 2009 to 130.132.248.62. Redistribution subject to AIP license or copyright; see http://jap.aip.org/jap/copyright.jsp

Supplementary Information for:
Effect of Spin-Polarized Electrons on THz Emission from Photoexcited GaAs

James M. Schleicher, Shayne M. Harrel, Charles A. Schmuttenmaer[a)]
Yale University, Department of Chemistry, 225 Prospect St., New Haven, CT 06520-8107 USA
[a)]Electronic mail: charles.Schmuttenmaer@yale.edu
December 21, 2008

This document contains additional material on the experimental apparatus, wafer orientation and definition of axes, generating spin-polarized electrons, excitation of GaAs(110) well above the bandgap, and additional polar plots.

Experimental apparatus

All data presented in this paper were recorded using the experimental setup described previously[1] and shown in Figure S1. Briefly, > 99% of laser intensity (1 kHz pulse train of ~100 fs pulses at ~800 mW average power) initiates a process that produces a THz pulse. The emission is detected by Free-Space Electrooptic Sampling (FSEOS) using a 1 mm thick ZnTe(110) crystal where the remaining < 1% of the optical beam serves as an optical gate.[2] Manipulation of the excitation beam polarization is achieved by placing a half- and quarter-wave plate (both zero-order) in the excitation beam path. A wire-grid polarizer that rejects vertically polarized THz radiation (not shown) is placed in front of the detector crystal to ensure maximum sensitivity towards horizontally polarized THz light. Data reported as a function of wave plate angle (as opposed to full THz waveforms) are obtained by monitoring only the peak of the waveform and averaging at least 500 points.

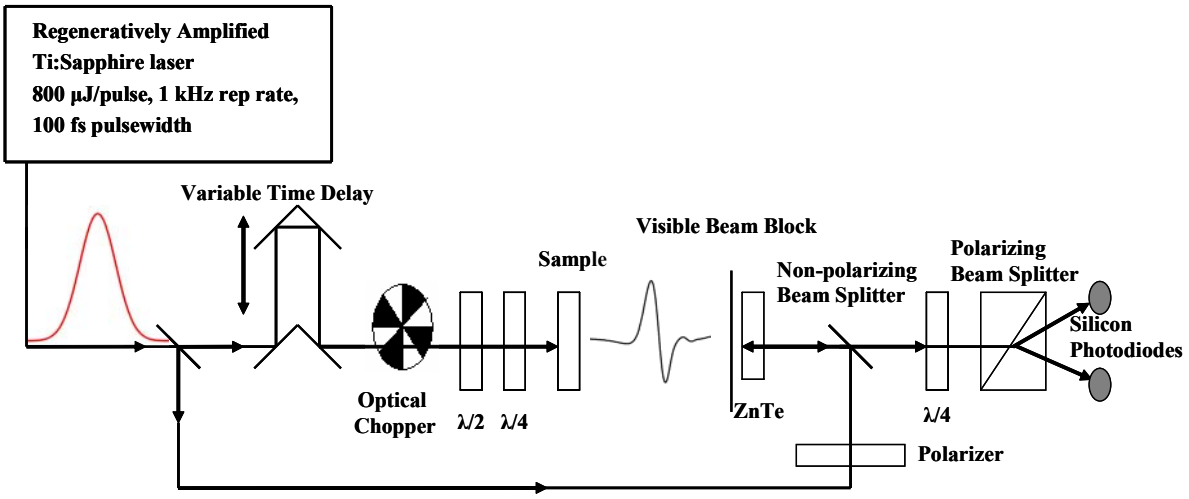

Fig. S1. Experimental Apparatus.

Wafer orientation and definition of axes

The X-emission for GaAs(111) is defined as the component of the THz emission that is parallel to the projection of the (100) axis onto the surface of the wafer, and for GaAs(110) the X-emission is defined as the component parallel to the (001) axis (see Figure S2). The Y-emission for both crystal faces is perpendicular to the X-emission.

In addition to rotating the sample by 90° to measure Y-emission, the quarter-wave plate is rotated 90° and the half-wave plate is rotated 45°. Both the sample and wave plates are rotated in the same direction. Rotating the sample and wave plates in this fashion is equivalent to rotating the detector in the opposite direction. The reason it is done in this manner is because the detector is polarization-sensitive and somewhat cumbersome to rotate.

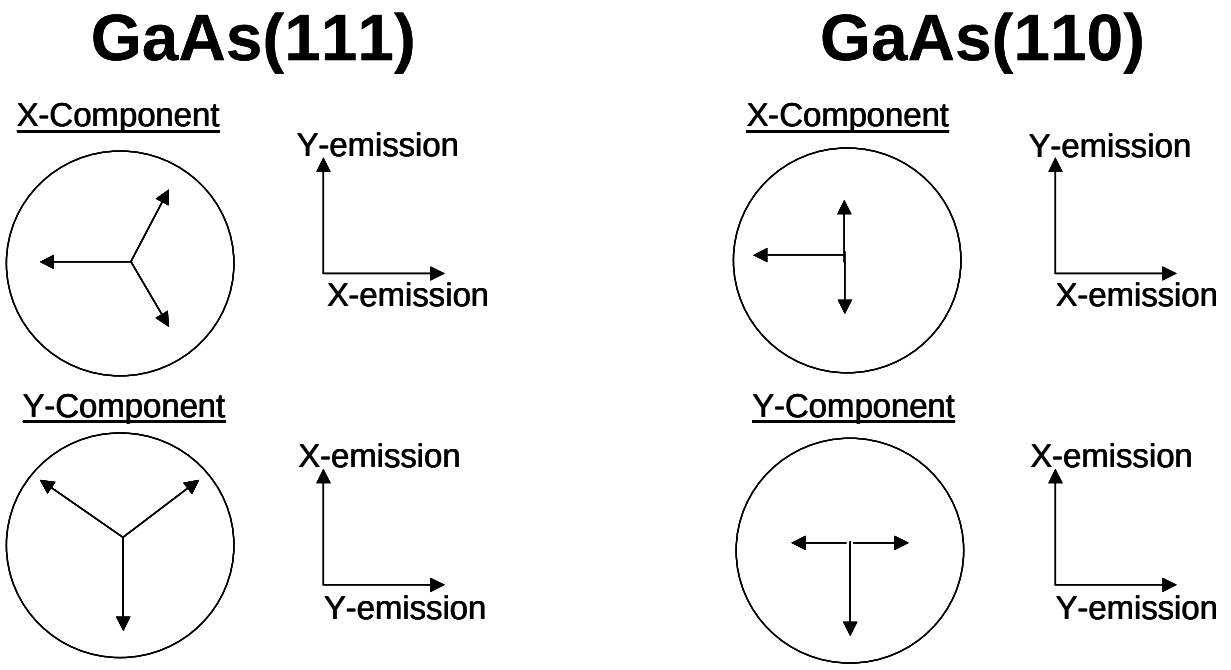

FIG. S2. Sample orientation scheme. On the left are the X- and Y-component orientations for a GaAs(111) wafer. The circle represents the wafer orientation in lab space, where the vectors are the projection of the crystallographic axes onto the surface of the wafer. The X-emission is parallel to one of these equivalent axis projections and the Y-emission is perpendicular. On the right are the X- and Y-component orientations for a GaAs(110) wafer. The X-emission is parallel to the projection of the (001) axis onto the surface and the Y-emission is perpendicular (parallel to the (100) and (010) axes).

Generating spin-polarized electrons

When exciting GaAs with light that is either elliptically or circularly polarized with photon energy 0.34 eV or less above the bandgap at the zone-center (i.e., between 1.43 eV and 1.77 eV at room temperature), an excess of spin-polarized electrons are generated.[3-5] This range of photon energies allows transitions to the conduction band from the light-hole and heavy-hole bands, but not from the split-off band. The net spin polarization orients itself parallel or anti-parallel to the propagation of the excitation beam. The selection rules in GaAs are such that when photoexciting with right-handed, circularly-polarized light, σ^+, and with a photon energy that falls between the $p_{3/2} \rightarrow s_{1/2}$ or $p_{1/2} \rightarrow s_{1/2}$ transitions (heavy-hole or light-hole to conduction band transitions) and the $s_{1/2} \rightarrow s_{1/2}$ transition (split-off band to conduction band), the resulting population of excited electrons will have a 50% excess of spin "forward" electrons (net spin pointing in the same direction as laser propagation), as seen in Figure S3.[3-5] The opposite holds true for σ^- light wherein a 50% excess of spin "backward" electrons is produced. Since our typical excitation wavelength is 800 nm (~1.55 eV photon energy), spin-polarized electrons are generated when exciting with circular polarization at room temperature. Also important for these studies is the fact that the spin-polarized electron population will vary sinusoidally as a function of the angle between the quarter-wave plate and the input beam's linear polarization, i.e., zero when it is linear, and a maximum amount when it is circular.

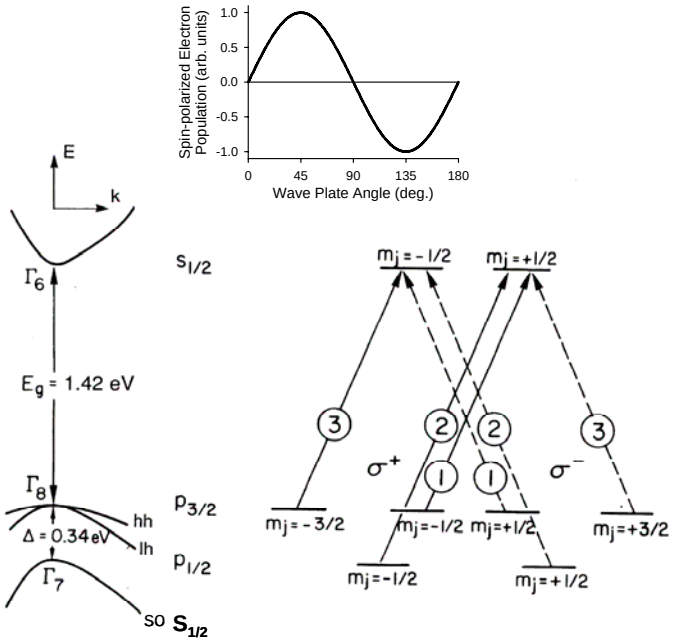

FIG. S3. The mechanism for generating spin-polarized electrons. Left: The energy gap of GaAs about the $k = 0$ point in momentum space. Bottom-right: The valence and conduction energy levels at $k = 0$ shown with their m_J quantum numbers. The allowed transitions for right-circularly polarized light (σ^+) are shown in solid lines and the allowed transitions for left-handed circularly polarized light (σ^-) are shown in dashed lines. The relative strength of each transition is represented by the number in the circle. Top: The relative population of spin-polarized electrons as a function of quarter-wave plate angle. Spin-polarized electrons are generated when electrons are promoted with circularly polarized light from the degenerate light-hole (lh) and heavy-hole (hh) bands, but not the split-off (so) band. Band diagram and optical transitions diagram are from Reference 5.

Excitation of GaAs(110) well above the bandgap

When exciting with 400 nm light, the dependence of THz emission from GaAs(110) as a function of quarter-wave plate angle agrees very well with the calculated behavior.

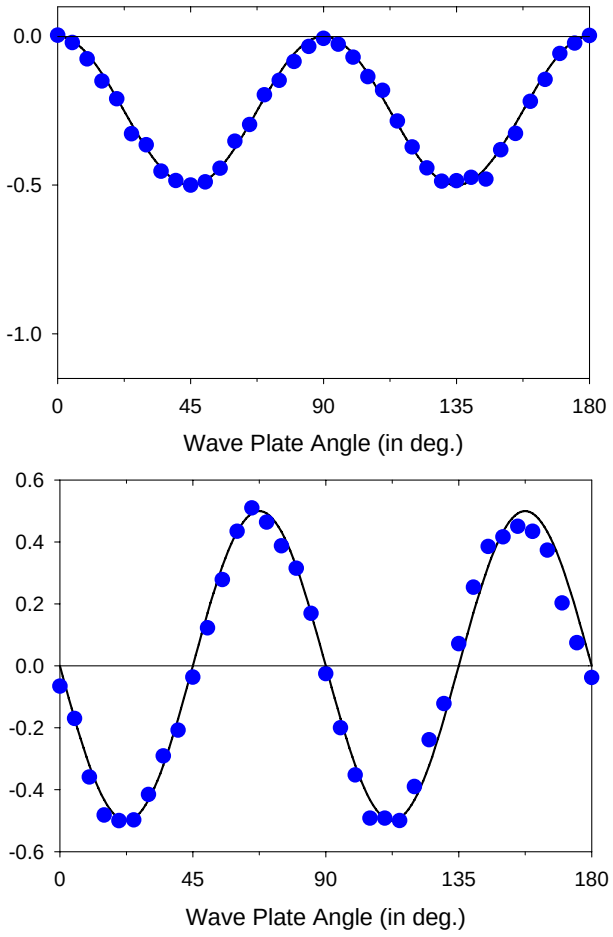

FIG. S4. (Color online) THz emission dependence on quarter-wave plate angle for excitation initially polarized parallel to the *x*-axis far above bandgap at 400 nm (blue circles), plotted with theoretical calculations (solid black curve). X/Above is the top plot and Y/Above is the bottom plot.

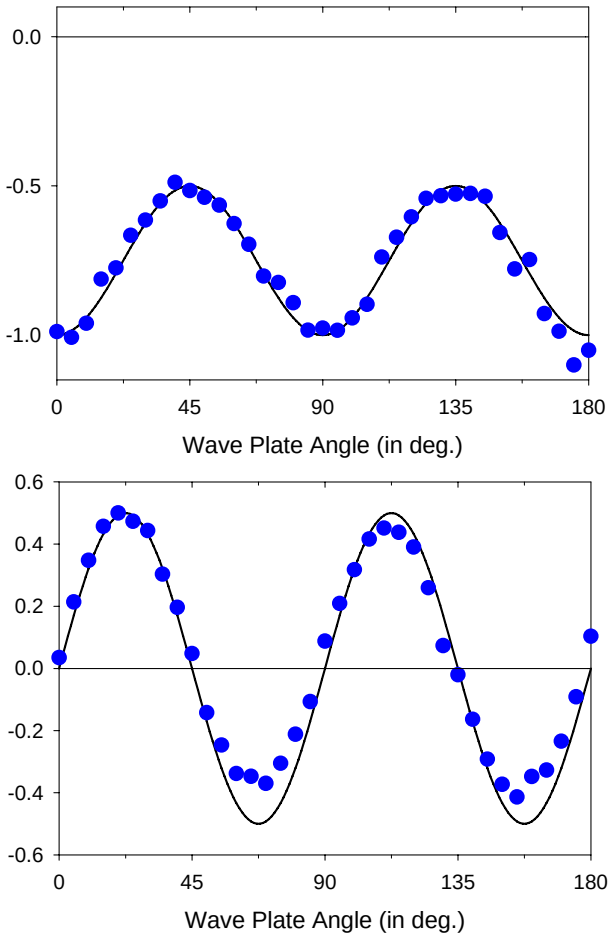

FIG. S5. (Color online) THz emission dependence on quarter-wave plate angle for excitation initially polarized perpendicular to the *x*-axis far above bandgap at 400 nm (blue circles), plotted with theoretical calculations (solid black curve). X/Above* is the top plot and Y/Above* is the bottom plot.

Polar plots

Figures S6, S7, and S8 are polar plots of the THz emission as a function of quarter-wave plate angle. Figure S6 shows the same data as in Figure of the main text. However, the deviations from the calculated behavior are not specified as in Figure 4 of the main text. Instead, thin arrows are used to indicate the direction of the data points as a function of quarter-wave plate angle. Figures S7 and S8 present polar plots for GaAs(110) with the linear polarization prior to the quarter-wave plat parallel or perpendicular to the X-emission axis, respectively.

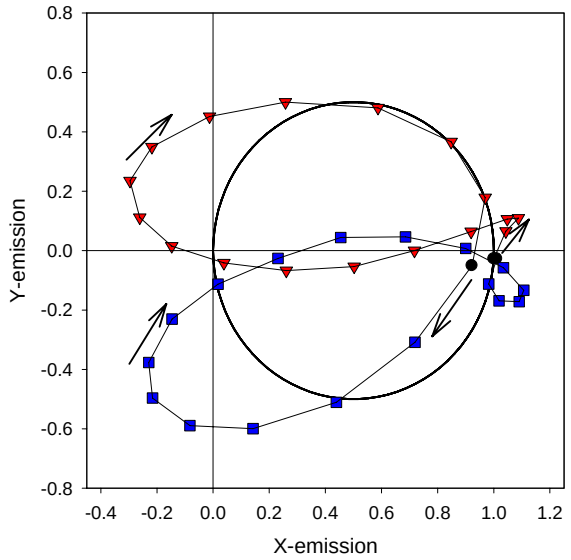

FIG. S6. (Color online) Polar plot representing the current within the plane of GaAs(111) as a quarter-wave plate is rotated. The thick solid black line forming a circle represents the calculated current: twice repeating, one full clockwise loop as the wave plate is rotated from 0° to 90°, and a second as it is rotated from 90° to 180°. Both begin and end at an X-emission of 1 and a Y-emission of 0. The red triangles represent right-handed excitation (wave plate angles 5° to 85°), blue squares represent left-handed excitation (95° to 175°), and black circles represent linear excitation (0°, 90°, and 180°). The thin line and arrows are present to guide the eye and for directionality.

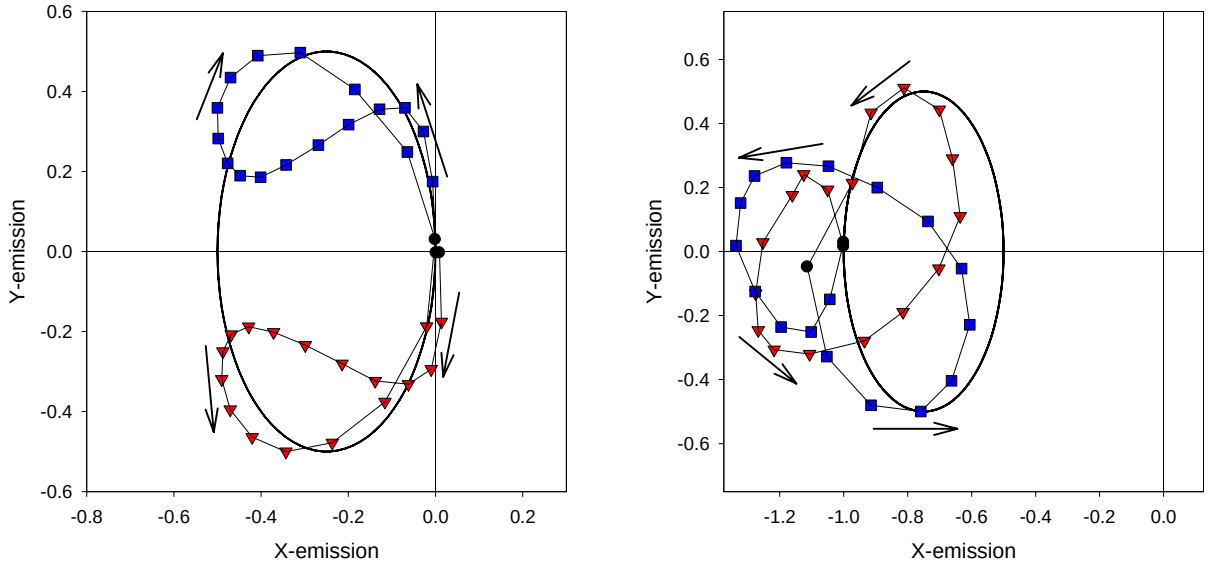

FIG. S7. (Color online) Left: Polar plot representing the current within the plane of GaAs(110) as a quarter-wave plate is rotated with initial excitation polarization parallel to the X-emission axis. Right: Polar plot representing the current within the plane of GaAs(110) as a quarter-wave plate is rotated with initial excitation polarization perpendicular to the X-emission axis. In both cases, the thick solid black line forming an ellipse represents the calculated current: twice repeating, one full clockwise loop as the wave plate is rotated from 0° to 90°, and a second as it is rotated from 90° to 180°. The parallel case begins and ends at an X-emission of 1 and a Y-emission of 0, while the perpendicular case begins and ends at an X-emission of -1 and a Y-emission of 0. The red triangles represent right-handed excitation (wave plate angles 5° to 85°), blue squares represent left-handed excitation (95° to 175°), and black circles represent linear excitation (0°, 90°, and 180°). The thin line and arrows are present to guide the eye and for directionality.

References

1. E. Beaurepaire, G. M. Turner, S. M. Harrel, M. C. Beard, J. Y. Bigot et al., "Coherent Terahertz Emission from Ferromagnetic Films Excited by Femtosecond Laser Pulses," Appl. Phys. Lett. **84** (18), 3465 (2004).
2. Q. Wu and X. C. Zhang, "Free-Space Electrooptic Sampling of Terahertz Beams," Appl. Phys. Lett. **67** (24), 3523 (1995).
3. G. Lampel, "Nuclear Dynamic Polarization by Optical Electronic Saturation and Optical Pumping in Semiconductors," Phys. Rev. Lett. **20** (10), 491 (1968).
4. D. T. Pierce and F. Meier, "Photoemission of Spin-Polarized Electrons from GaAs," Phys. Rev. B **13** (12), 5484 (1976).
5. D. T. Pierce, R. J. Celotta, G. C. Wang, W. N. Unertl, A. Galejs et al., "GaAs Spin Polarized Electron Source," Rev. Sci. Instrum. **51** (4), 478 (1980).